The Astrophysical Journal Letters, 743:L12 (6pp), 2011 December 10 doi:10.1088/2041-8205/743/1/L12

KEPLER OBSERVATIONS OF RAPID OPTICAL VARIABILITY IN ACTIVE GALACTIC NUCLEI

R. F. Mushotzky[1,2], R. Edelson[1], W. Baumgartner[2], and P. Gandhi[3]
[1] Department of Astronomy, University of Maryland, College Park, MD 20742, USA; richard@astro.umd.edu
[2] Laboratory for High Energy Astrophysics, NASA/GSFC, Code 662, Greenbelt, MD 20771, USA
[3] Institute of Space and Astronautical Science, Japan Aerospace Exploration Agency, 3-1-1 Yoshinodai, chuo-ku, Sagamihara, Kanagawa 252-5210, Japan
Received 2011 September 19; accepted 2011 October 31; published 2011 November 18

ABSTRACT

Over three quarters in 2010–2011, *Kepler* monitored optical emission from four active galactic nuclei (AGNs) with ∼30 minute sampling, >90% duty cycle, and $\lesssim$0.1% repeatability. These data determined the AGN optical fluctuation power spectral density (PSD) functions over a wide range in temporal frequency. Fits to these PSDs yielded power-law slopes of −2.6 to −3.3, much steeper than typically seen in the X-rays. We find evidence that individual AGNs exhibit intrinsically different PSD slopes. The steep PSD fits are a challenge to recent AGN variability models but seem consistent with first-order magnetorotational instability theoretical calculations of accretion disk fluctuations.

Key words: accretion, accretion disks – black hole physics – galaxies: active – galaxies: Seyfert

Online-only material: color figures

1. INTRODUCTION

The optical continuum from active galactic nuclei (AGNs) is believed to be dominated by emission from an accretion disk surrounding a supermassive black hole and can be adequately modeled as radiation from a simple Shakura–Sunyaev disk (Edelson & Malkan 1986). Because this region is too small to image (except via gravitational lensing; Kochanek 2004), indirect methods must be used to probe its structure and physical conditions. One of the best probes is provided by the strong variability seen throughout the optical/ultraviolet/X-ray bands in most AGNs. However, limitations with many ground-based optical observations have made it difficult to obtain accurate, densely, and regularly sampled data sets covering the large range of timescales necessary to constrain disk physics and search for characteristic times which may be related to orbital, dynamic, or other expected timescales. In particular, diurnal and weather-related interruptions can severely degrade the ground-based sampling pattern and atmospheric seeing introduces photometric errors that are much larger than the *Kepler* uncertainties and often are as large as or larger than the intrinsic short timescale optical source variability. However, ground-based data have sampled much longer timescales than are available in the present *Kepler* data sets.

The natural timescales for a disk—light-crossing ($t_{\rm l}$), dynamical ($t_{\rm dyn}$), and thermal ($t_{\rm th}$) timescales—are set by the black hole mass and the accretion processes (Frank et al. 2002). The order of magnitude estimates for these timescales are $t_{\rm l} = 2.6\,M_7\,R_{100}$ hr, $t_{\rm dyn} = 10\,M_7\,{R_{100}}^{3/2}$ days, $t_{\rm th} = 0.46\,M_7\,{R_{100}}^{3/2}\,{\alpha_{0.01}}^{-1}$ yr, where M_7 is the black hole mass in units of $10^7\,M_\odot$, R_{100} is the emission distance in units of 100 times the Schwarzschild radius $2GM/c^2$, and $\alpha_{0.01}$ is the Shakura–Sunyaev viscosity parameter (Shakura & Sunyaev 1973) divided by 100. For assumed Eddington ratios of 0.01–0.1 and mass ranges of 10^6–$10^9\,M_\odot$, typical for AGNs, these natural timescales range from hours to years. Previous data have been unable to constrain the optical time variability over this wide range for any individual AGN.

The *Kepler* mission (Borucki et al. 2010) provides a solution to these observational difficulties. *Kepler* has been observing a ∼115 deg^2 region of sky, monitoring ∼165,000 sources every 29.4 minutes with unprecedented stability ($\lesssim$0.1% for a 15th magnitude source) and high (>90%) duty cycle over a period of years. During Q6 (Quarter 6; UT 2010 June 24–September 22), Q7 (2010 September 23–December 22), and Q8 (2010 December 22–2011 March 24), the *Kepler* target list included at least four variable AGNs from our guest observer program. This Letter reports initial results of Q6–Q8 (and in one instance Q4) observations of these *Kepler* AGNs, focusing on fluctuation power spectral density (PSD) analysis. The source selection, data collection, and reduction are given in Section 2; the time series analysis and results are reported in Section 3; implications are discussed in Section 4; and brief conclusions are given in Section 5.

2. DATA

2.1. Source Selection

Because it lies at low galactic latitudes not systematically covered by major extragalactic/AGN surveys, the *Kepler* field (∼0.3% of the sky) currently contains only a few cataloged AGNs. (Note however that a portion of the *Kepler* field is covered by the Sloan Digital Sky Survey (SDSS)/SEGUE.[4]) Targets must be identified and windows chosen before *Kepler* data can be downloaded. Thus, we have undertaken extensive efforts to identify AGNs in the *Kepler* field. This started with a database search to find previously identified AGNs. We then applied the method of Stocke et al. (1983) to the *ROSAT* All Sky Survey (RASS; Voges et al. 1999) to select AGN candidates based on their X-ray-to-optical flux ratio. We also used the Two Micron All Sky Survey (2MASS) all-sky survey catalog (Strutskie et al. 2006) to identify AGN candidates based on infrared colors (Malkan 2004) and association with a RASS source.

Table 1 gives details of the "*Kepler* AGN" whose light curves are presented in this Letter, a sample of four variable AGNs that *Kepler* has been observing since Q6. Of these four, only Zw 229−15 ($z = 0.0275$; Falco et al. 1999; Proust 1990) had been identified as an AGN prior to the launch of *Kepler*. A recent reverberation mapping campaign found it had an Hβ lag of ∼4 days and estimated its black hole mass at $\sim 10^7\,M_\odot$ (Barth

[4] http://www.sdss.org/segue/

Table 1
Kepler AGN Source Parameters

Source Name	*Kepler* ID	R.A.	Decl.	z	RASS
Zw 229-15	6932990	19 05 26.0	+42 27 40	0.028	0.450
KA 1925+50	12158940	19 25 02.2	+50 43 14	0.067	0.170
KA 1858+48	11178007	18 58 01.1	+48 50 23	0.079	0.210
KA 1904+37	2694185	19 04 58.7	+37 55 41	0.089	0.023

Note. Columns 1 and 2 give the source name (KA refers to newly discovered "*Kepler* AGN" first reported in this Letter) and *Kepler* ID number, Columns 3 and 4 give the position, Column 5 the redshift, and Column 6 the *ROSAT* All Sky Survey (RASS) count rate in counts s^{-1}.

et al. 2011). The other three AGNs in Table 1 were all discovered as a result of the search described above. (The prefix "KA" is used to designate newly identified *Kepler* AGNs.) Spectra of these three plus ten other newly discovered *Kepler* AGNs are given in R. Edelson & M. Malkan (2011, in preparation).

2.2. Kepler SAP Light Curves

The *Kepler* standard data processing pipeline (Jenkins et al. 2010) operates on original spacecraft data to produce calibrated pixel data (Quintana et al. 2010). The next step, PA, uses simple aperture photometry to extract "SAP_FLUX" count rates from these two-dimensional images (Twicken et al. 2011). The spacecraft does not download full CCD frames but only "postage stamp" images for the targets. Only a fraction of the downloaded pixels are used in the extraction. The next step in the standard pipeline, SAPPDC, conditions the light curves for transit searches, outputting PDC_FLUX light curves. However, no conditioning occurred for sources presented in this Letter (the SAP_FLUX and PDC_FLUX data are identical to within a constant offset), so this and all further steps are not relevant to the current work. We use SAP_FLUX count rates for our AGN light curve analyses. These light curves are presented in Figures 1 and 2.

Kepler, with its $\lesssim$0.1% repeatability, >90% duty cycle, and durations of years, explores a level of data quality superior to anything previously obtained. Thus, one must be concerned about other sources of error, especially systematic errors, in this relatively young mission. An independent check of the *Kepler* data is available for Zw229−15 since in 2010, it was observed by both *Kepler* and the ground-based Lick AGN Monitoring Program (LAMP). These light curves, shown in Figure 1, indicate a very good agreement between *Kepler* and independent ground-based LAMP data, well within the LAMP $\sim$ 1% errors and so, at least in this case, the systematic and other errors in the Zw 229−15 data are generally no larger than the $\sim$1% LAMP errors.

However, the quoted *Kepler* errors are much smaller, and there is currently no way to be sure that systematic errors are not affecting the data at the level between $\sim$0.1% and $\sim$1%. Indeed, Figure 2 shows that small, short-term (1–2 days), discontinuities are sometimes observed following monthly data downloads or safe-mode events. This is believed to arise from thermally induced focus changes as the solar illumination changes during spacecraft slews.[5] Both our group and the *Kepler* team are working to correct for this in future analyses. While our understanding will undoubtedly improve as the mission progresses at this stage, all that can be done at this time is to remind the reader that this, as well as other (currently unknown), systematic error could still be present in these data.

[5] http://archive.stsci.edu/kepler/release_notes/release_notes5/Data_Release_05_2010060414.pdf.

Table 2
Kepler AGN Quarterly Observations

Source Name	Quarter	10^3 counts s^{-1}	err_dir	err_ind	α
Zw 229−15	Q4	12.1	0.047%	0.065%	−3.05
Zw 229−15	Q6	12.0	0.051%	0.068%	−3.31
Zw 229−15	Q7	12.9	0.046%	0.062%	−3.14
Zw 229−15	Q8	10.4	0.052%	0.055%	−2.96
KA 1925+50	Q6	4.2	0.071%	0.084%	−2.60
KA 1925+50	Q7	3.8	0.065%	0.081%	−2.75
KA 1925+50	Q8	4.1	0.075%	0.078%	−2.67
KA 1858+48	Q6	2.1	0.117%	0.159%	−2.87
KA 1858+48	Q7	1.3	0.128%	0.207%	−2.97
KA 1904+37	Q7	5.8	0.071%	0.097%	−2.74
KA 1904+37	Q8	5.5	0.080%	0.087%	−2.95

Notes. Columns 1 and 2 give the source name and quarter, Column 3 gives the mean SAP_FLUX count rate in 10^3 counts s^{-1}, and Column 4 gives the ratio of the mean quoted errors divided by the mean flux. Column 5 gives the error rate derived from the PSD fits as discussed in Section 3. Column 6 gives the fitted PSD slopes (α) for each quarter.

3. POWER SPECTRAL DENSITY FUNCTIONS

3.1. PSD Measurement

The optical flux variations in AGNs are aperiodic. A standard tool for characterizing such broadband (in temporal frequency) variability is the periodogram, which measures the fluctuation PSD function. AGN PSDs have been best studied in the X-rays, where the PSDs show a broad shape that has been simply characterized as a double power law that breaks from a steep red noise high-frequency slope $\alpha_H \sim -2$ ($S \propto f^{\alpha}$, where α is the slope, S is the spectral density, and f is the temporal frequency) to a flatter low-frequency slope $\alpha_L \sim -1$, at a break frequency f_b that typically corresponds to timescales of order of a week, but scales with the mass of the black hole (e.g., Edelson & Nandra 1999; Uttley et al. 2002; Markowitz et al. 2003).

We used the *Kepler* SAP data to measure PSDs for all of these *Kepler* AGNs. Currently, large photometric offsets introduced by quarterly spacecraft rolls prevent data from being combined across quarters, so these PSDs only cover individual quarters. This problem should eventually be solved, so we will produce PSDs covering longer timescales in a future paper.

For each light curve, a first-order function was subtracted off so that the first and last points of the light curve were equal. This "end-matching" reduces artificial flattening due to leakage (Fougere 1985). This correction steepens the slopes by a mean value of 0.7, 0.3, 0.8, and 0.7 for Zw 229−15, KA 1925+50, KA 1858+48, and KA 1904+37, respectively. Fractional normalization was used, so the resulting power density has units of rms^2 Hz^{-1}.

The resulting PSDs (see Figure 3), fitted with a single power law ($S \propto f^{\alpha}$) plus noise model on temporal frequencies of $\sim 4 \times 10^{-7}$ to $\sim 4 \times 10^{-5}$ Hz (corresponding to timescales of $\sim$6 hr to $\sim$1 month), are very steep with slopes from $\alpha = -2.6$ to -3.3.

3.2. Error Analysis

These PSDs also allow a check of the true noise level in the light curves. The fractional error (err_dir = $\langle \mathrm{err} \rangle / \langle \mathrm{flux} \rangle$) is reported in Column 4 of Table 2. Using the formula of Vaughan

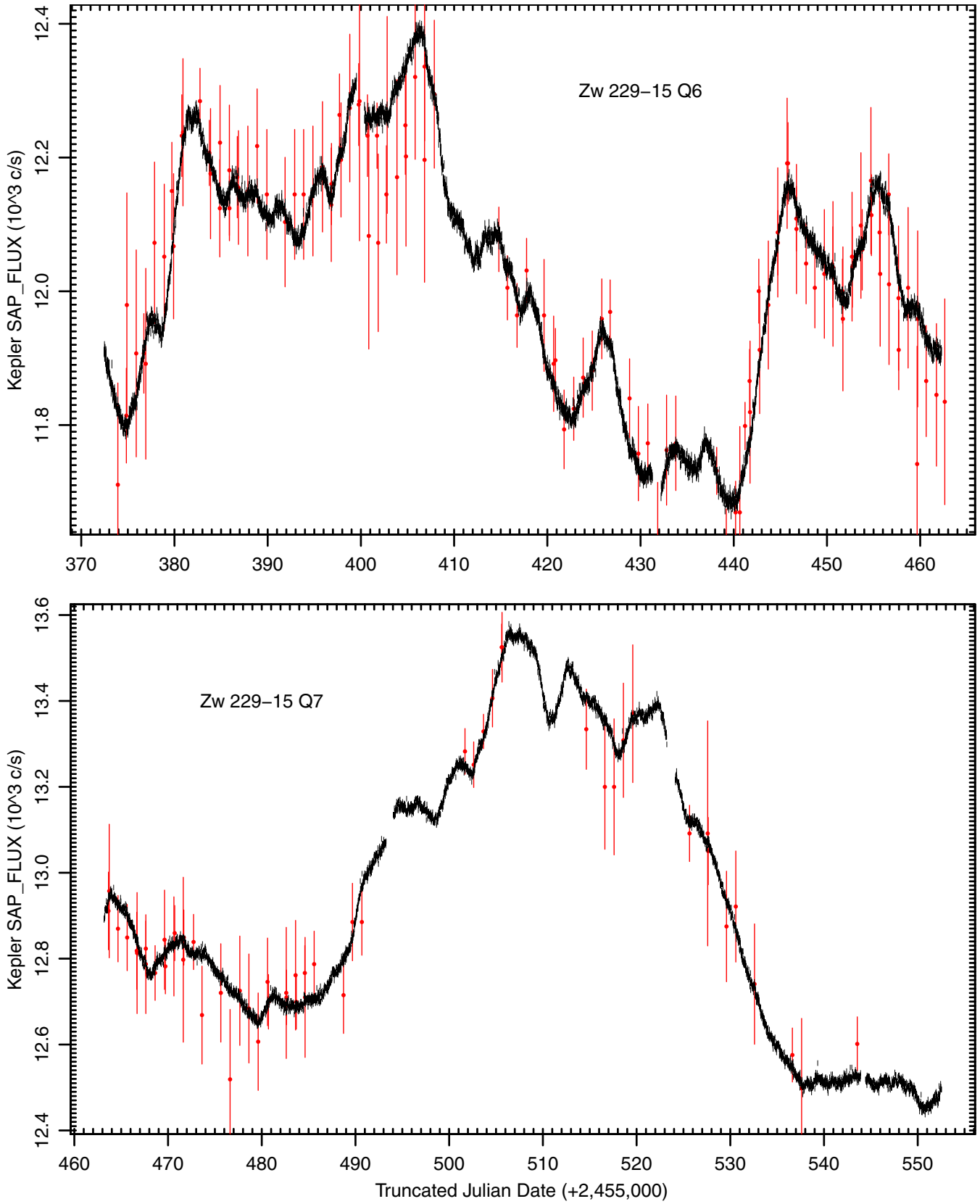

Figure 1. *Kepler* Q6 (top) and Q7 (bottom) light curves of the narrow-line Seyfert 1 galaxy Zw 229−15 (in black). Each panel contains over 4200 cadences, gathered one every ∼30 minutes, with a precision of ∼0.1%; a typical error bar can be is seen in the outlier at TJD ∼ 539. There are monthly ∼1 day data download gaps (e.g., TJD ∼ 431 and 524), but the overall duty cycle is >90%. Note that the ∼8% flux discontinuity between Q6 and Q7 as the quarterly spacecraft roll moves the source onto a different chip and a new SAP aperture is used. Note also the excellent agreement with simultaneous ground-based LAMP data (shown in red; Barth et al. 2011), scaled to account for different aperture sizes.

(A color version of this figure is available in the online journal.)

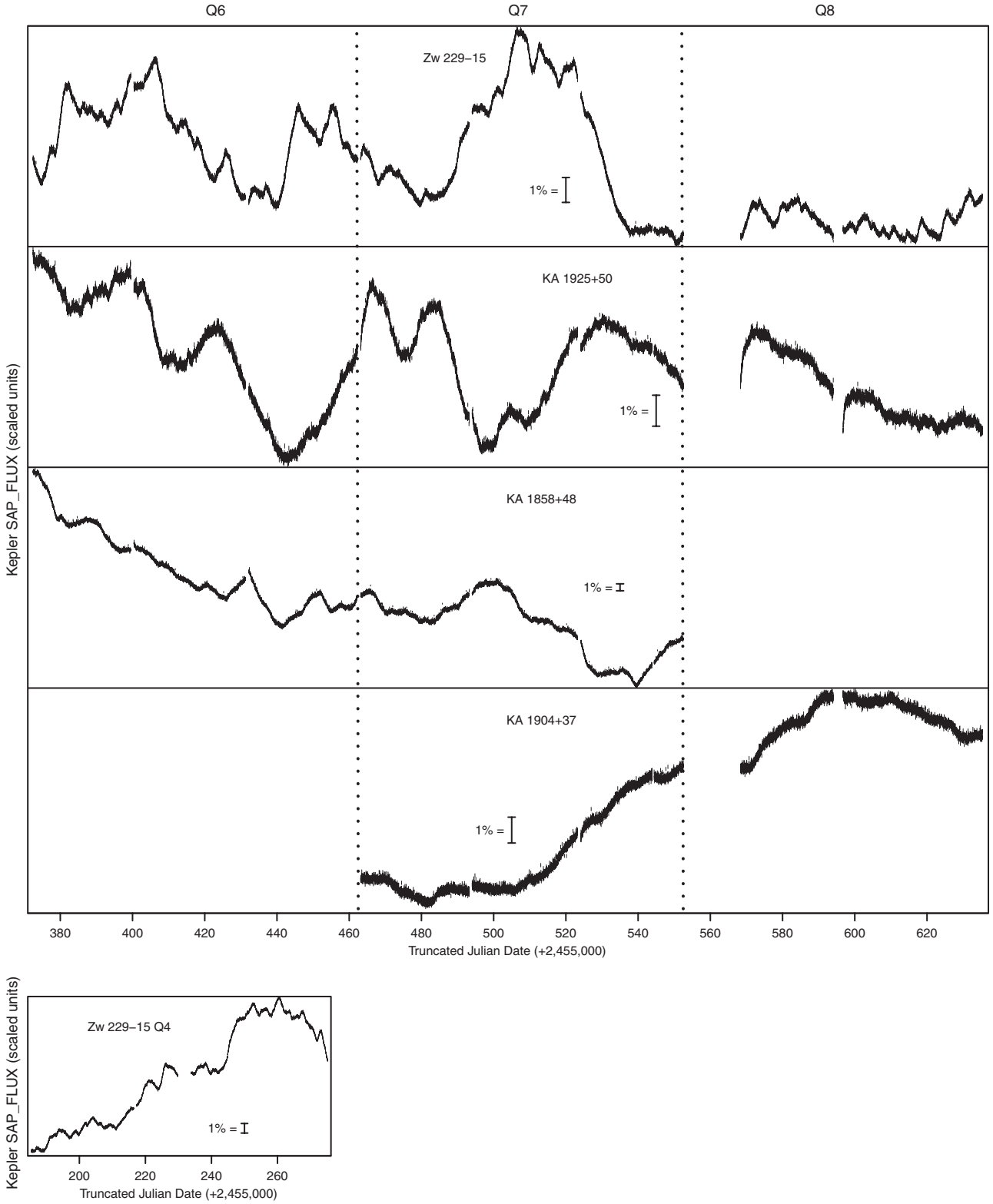

Figure 2. (a) Q6–Q8 light curves for four variable *Kepler* AGNs. A 1% bar is shown for scale. Q8 data were not obtained for KA 1858+48 because it fell on the defective Module 3. *Kepler* observations of KA 1904+37 did not begin until Q7. Arbitrary offsets have been applied to match light curves across quarterly transitions (the dotted lines at TJD ∼ 462 and 552). Note the 16 day gap due to a safe-mode event at the beginning of Q8; this makes the offset for that quarter highly uncertain. Note also that light curves occasionally show ∼1% discontinuities immediately following monthly data downloads or safe-mode events (e.g., TJD ∼ 568 and 586 in KA 1925+50, and TJD ∼ 432 in Zw 229−15 and KA 1858+48) due to thermally induced focus changes. (b) Same as panel (a) but for the Zw 229−15 Q4 data.

et al. (2003), we derived err_ind = sqrt($\langle err^2 \rangle / \langle flux \rangle^2$) from the PSD, given in Column 5. This reduces to the same quantity ($\langle err \rangle / \langle flux \rangle$) in the limit of small fluctuations in the fluxes and errors, as is the case with these data. The errors derived from the PSD analysis are typically ∼25% larger than the quoted light curve errors. This indicates that the quoted errors are slightly underestimated and that no other source of systematics dominates the quoted errors.

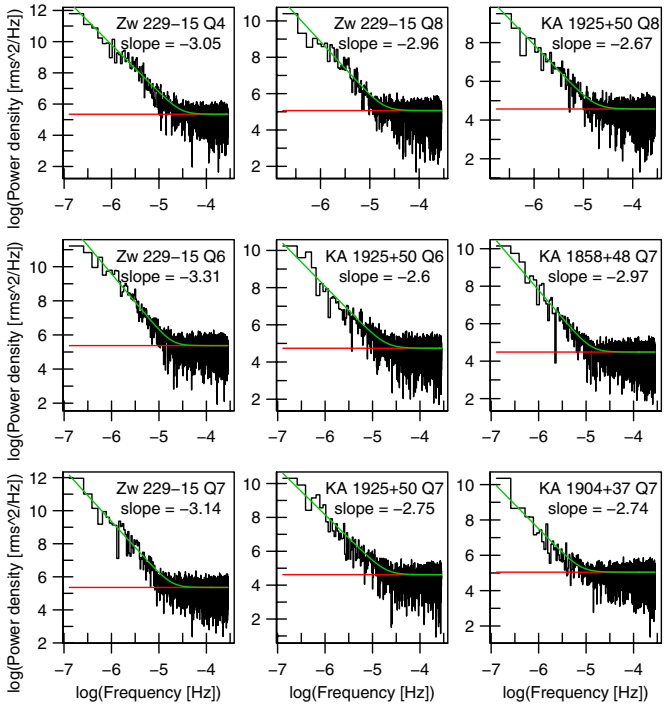

Figure 3. Optical PSDs and power-law plus white noise fits for the four AGNs in selected quarters over temporal frequencies ∼10–6.5 to 10–3.5 Hz. The fits are shown in green and the noise level in red. Source name, quarter, and fitted power-law slope (a) are given in the upper right of each plot.

(A color version of this figure is available in the online journal.)

The PSD slopes for each quarter (listed in Table 2) show small scatter for individual objects. It is difficult to directly measure reliable errors on derived PSD slopes, but an estimate is provided by the observed dispersion for individual objects. For the two sources with the most data, Zw 229−15 and KA 1925+50, the mean slope and associated standard deviations are ⟨alpha⟩ = −3.11 ± 0.15 and −2.67 ± 0.08. These differ by ∼2.5 standard deviations, suggesting, at very marginal significance, that the intrinsic difference between the derived slopes for these objects is larger than the associated errors. (The quoted uncertainties are standard deviations of the distributions of the PSD slopes for different quarters) Note that without the red noise leak correction, the standard deviations for these two sources would have been 0.58 and 0.22, respectively, so our correction successfully reproduces similar PSD slopes between the various quarters for each source. Since PSD analyses are notoriously susceptible to analytical systematics (see, e.g., Vaughan et al. 2003) and there is the possibility that currently unknown systematic errors could affect these new *Kepler* data (see Section 2.2), the agreement in slope from quarter to quarter provides a degree of confidence that the observed steep slopes are accurate.

4. DISCUSSION

4.1. Comparison to Previous Results

4.1.1. Optical Data

Kepler light curves are of much higher quality and sampling rate than previous data. For example: in the data used by Kelly et al. (2009) the highest photometric quality is from the MACHO survey of Geha et al. (2003) which has ∼5% photometric errors and 600 good photometric measurements over 7.5 yr, and thus samples at ∼1 point every 4.5 days compared to the 0.1% *Kepler* errors and 1 data point roughly every 30 minutes. Previous attempts to derive the PSD over a wide range of timescales have had to combine the data from many objects and several surveys (Hawkins 2002) or have relied on relatively sparsely sampled data, from several different telescopes (Breedt et al. 2010).

Previous results (e.g., Kelly et al. 2009) tend to find best-fitting PSDs with slopes of ∼−1.8 for the collective sample, rather flatter than what we have found. Since the *Kepler* PSDs cannot continue to very low frequencies with such steep slopes without implying very large variability amplitudes, there must be a break at timescales >1 month, which may make the *Kepler* PSDs consistent with previous work. It is not surprising that the results of our observations are rather different from what has been published previously—the other observations could not see the effects we are detecting. While there is a formal overlap in sampled timescales between our *Kepler* and other data, the much larger error bars for the previous PSDs (e.g., Breedt et al. 2010) at characteristic frequencies above ∼a few $\times 10^{-5}$ Hz makes comparison difficult. However, for at least one object, NGC 4051 (Breedt et al. 2010), the observed PSD in the 10^{-6} Hz $\times 10^{-8}$ Hz is well determined and is flatter than our *Kepler* results for all of our objects. One possible explanation for the differences may lie in the different luminosities or Eddington ratios of the objects, since NGC 4051 is significantly less luminous and probably less massive than the objects in our sample.

4.1.2. X-Ray Data

Although the particular Seyfert 1s in our sample do not have measured X-ray PSDs, many other Seyfert 1s have had X-ray PSDs measured over these timescales. These are always much flatter, typically having high frequency slopes of −1 to −2 (Edelson & Nandra 1999; Uttley et al. 2002; Markowitz et al. 2003). Thus, our measurement of steep optical PSDs on short timescales is somewhat surprising because it is so different from that measured in the X-rays, and because Seyfert 1 optical and X-ray light curves appear to track well, at least on longer timescales (Uttley et al. 2003).

4.2. Physical Implications for Accretion Disks

The characteristic timescales of the fluctuations should correspond to different physical mechanisms which may be related to the size of the system, the dynamical timescales, epicyclic frequencies, g-modes, or other characteristic timescales that may influence the source of the variance. Since the source of the accreting material in AGNs is not known, it is unclear if the source of the perturbations is changes in the accretion flow, the turbulence due to physics in the disk itself (from the magnetorotational instability (MRI) mechanism, e.g., Reynolds & Miller 2009b; Noble & Krolik 2009), or perhaps other physics. As shown by McHardy et al. (2006), the characteristic timescale seen in the X-ray PSDs is related to the AGN mass and the accretion rate. However, it is not known if this is also true for the optical PSDs (MacLeod et al. 2010).

Recent ground-based optical observations (e.g., Kelly et al. 2009, MacLeod et al. 2010) are consistent with a damped random walk model. However those light curves are sampled irregularly and more sparsely than these *Kepler* data (see Figure 2 in Kozlowski et al. 2010). Our PSDs are not consistent with the predicted high-frequency slope of −2. However, since there is very little overlap in frequencies and our sample size is much smaller direct comparison is difficult. Our data are just

capable of reaching the light travel time size of the disks on our sampled AGNs. The effective size of the region emitting radiation at a given frequency is (Baganoff & Malkan 1995)

$$r_{1/2} = 7.5 \times 10^{23} \varepsilon^{-1/3} \nu^{-4/3} (M/M_{\odot})^{-1/3} (L/L_{\rm Edd})^{1/3} r_{\rm G},$$

where $r_{\rm G}$ is the Schwarzschild radius, ε is the accretion efficiency, and ν is the effective observing frequency of the data. Utilizing an effective wavelength of 5000 Å, mass of $1 \times 10^7\, M_{\odot}$ (Barth et al. 2011), and Eddington ratio of 0.05 we find an effective light travel time ($r_{1/2}/c$) of ∼1 day which is close to our white noise limit of 0.25 days. The four sources in this Letter span only one order of magnitude in X-ray luminosity ($\log L(x) = 42.6$–43.6) and thus, probably, a small range in mass. In principle, it is possible to use magnetohydrodynamic (MHD) calculations to estimate the shape and slope of the PSD expected from fluctuations within accretion disks. Although such modeling is still in its early days, several estimates of the expected PSD slopes are currently available. In these models the underlying physical drivers for variability in the light curve are variations in the accretion rate caused by the chaotic character of MHD turbulence. Noble & Krolik (2009) simulate emission from the coronae appropriate to the X-ray emission and thus it is not clear if their simulation is appropriate for our results and Chan et al. (2009) focus on Sgr A* which seems to be accreting in a different mode than the Seyfert 1s in our sample. Reynolds & Miller (2009a) show PSDs of the mass accretion rate whose high frequency slopes ∼−2.9, very close to those seen in our observations. However, their simulation was only run for a relatively short time ($\sim 1.2 \times 10^4\ GM/c^3$) which corresponds to 14 days for objects of the mass of Zw 229−15.

All simulations so far suffer from the fundamental problem that to compare them with observations, one has to convert the simulated disk characteristics into a radiation flux spectrum and thus it is not clear that the proxies for emission developed so far are appropriate. This problem is fully recognized by the simulators and thus, in general, they have been loath to directly compare to the data.

5. CONCLUSIONS

Power spectral analysis of four AGNs observed by *Kepler* during Q6–Q8 show very steep ($\alpha \sim -2.6$ to -3.1) slopes, considerably steeper than that seen in the X-rays. The PSDs for each source are consistent from quarter to quarter and, at $>2\sigma$ confidence, are different from each other. Analysis of these high quality light curves indicates that the influence of systematic errors is rather small; additionally, direct comparison of *Kepler* and LAMP monitoring of Zw 229−15 shows excellent agreement. Comparison with analytic models of AGN variability shows steeper than predicted slopes; however, comparison with MHD simulations seems to show better agreement. Further analysis of other characteristics of the light curve, longer time series, the analysis of more objects, and the comparison to semi-analytic models of time variability will be the subject of future papers. We hope that these new high quality *Kepler* data will stimulate the calculation of the time series from accretion disks.

We thank the *Kepler* team for their efforts to make the data accessible and tractable and the *Kepler* GO program for funding, Matt Malkan for extensive contributions to the identification of new *Kepler* AGNs, Simon Vaughan for valuable help with PSD measurements, and Aaron Barth and the LAMP team for early access to their data.

REFERENCES

Baganoff, F. K., & Malkan, M. A. 1995, ApJ, 444, L13
Barth, A., Nguyen, M. L., Malkan, M. A., et al. 2011, ApJ, 732, 121
Borucki, W., Koch, D., Basri, G., et al. 2010, Science, 327, 977
Breedt, E., Arévalo, P., McHardy, I. M., et al. 2010, MNRAS, 394, 427
Chan, C.-K., Liu, S., Fryer, C. L., et al. 2009, ApJ, 701, 521
Edelson, R., & Malkan, M. A. 1986, ApJ, 308, 59
Edelson, R., & Nandra, K. 1999, ApJ, 514, 682
Falco, E., Kurtz, M. J., Geller, M. J., et al. 1999, PASP, 111, 438
Fougere, P. 1985, J. Geophys. Res., 90, 4355
Frank, J., King, A. R., & Raine, D. J. 2002, Accretion Power in Astrophysics (Cambridge: Cambridge Univ. Press)
Geha, M., Alcock, C., Allsman, R. A., et al. 2003, AJ, 125, 1
Hawkins, M. R. S. 2002, MNRAS, 329, 76
Jenkins, J. M., Caldwell, D. A., Chandrasekaran, H., et al. 2010, ApJ, 713, L87
Kelly, B. C., Bechtold, J., & Siemiginowska, A. 2009, ApJ, 698, 895
Kochanek, C. S. 2004, ApJ, 605, 58
Kozlowski, S., Kochanek, C. S., Udalski, A., et al. 2010, ApJ, 708, 927
MacLeod, C. L., Ivezić, Ž., Kochanek, C. S., et al. 2010, ApJ, 721, 1014
Malkan, M. 2004, in ASP Conf. Ser. 311, AGN Physics with the Sloan Digital Sky Survey, ed. G. T. Richards & P. B. Hall (San Francisco, CA: ASP), 449
Markowitz, A., Edelson, R., Vaughan, S., et al. 2003, ApJ, 593, 96
McHardy, I. M., Koerding, E., Knigge, C., Uttley, P., & Fender, R. P. 2006, Nature, 444, 730
Noble, S. C., & Krolik, J. 2009, ApJ, 703, 964
Proust, D. 1990, IAU Circ., 5134, 2
Quintana, E., Jenkins, J. M., Clarke, B. D., et al. 2010, Proc. SPIE, 7740, 77401X
Reynolds, C. S., & Miller, M. C. 2009a, ApJ, 692, 869
Reynolds, C. S., & Miller, M. C. 2009b, ApJ, 693, 1100
Shakura, N. I., & Sunyaev, R. A 1973, A&A, 24, 337
Stocke, J., Liebert, J., Gioia, I. M., et al. 1983, ApJ, 273, 458
Strutskie, M., Cutri, R. M., Stiening, R., et al. 2006, AJ, 131, 1163
Twicken, J., et al. 2011, Proc. SPIE, 7740, 77400J
Uttley, P., McHardy, I. M., & Papadakis, I. E. 2002, MNRAS, 332, 231
Uttley, P., Edelson, R., McHardy, I., Peterson, B., & Markowitz, A. 2003, ApJ, 584, L53
Vaughan, S., Edelson, R., Warwick, R., & Uttley, P. 2003, MNRAS, 345, 1271
Voges, W., Aschenbach, B., Boller, T., et al. 1999, A&A, 349, 389